

MOL #24398

A Molecular Mechanism of Pyruvate Protection against Cytotoxicity of Reactive Oxygen Species in Osteoblasts

Eiichi Hinoi, Takeshi Takarada, Yuriko Tsuchihashi, Sayumi Fujimori, Nobuaki Moriguchi, Liyang Wang, Kyosuke Uno and Yukio Yoneda

Laboratory of Molecular Pharmacology, Division of Pharmaceutical Sciences, Kanazawa University Graduate School of Natural Science and Technology, Kanazawa, Ishikawa 920-1192 (E.H., T.T., Y.T., S.F., N.M., L.W., K.Y., Y.Y.) and Taiko Pharmaceutical Co. Ltd., Suita, Osaka 564-0032 (N.M.), Japan

Running title: pyruvate prevents bone loss

*Corresponding author:

Dr. Yukio Yoneda

Laboratory of Molecular Pharmacology

Division of Pharmaceutical Sciences

Kanazawa University Graduate School of Natural Science and Technology

Kakuma-machi, Kanazawa, Ishikawa 920-1192, Japan

Tel/Fax, 81-(0)76-234-4471; E-mail, yyoneda@p.kanazawa-u.ac.jp

Text pages: 31

Tables: 0

Figures: 9

References: 27

Number of words: Total, 7,696; Abstract, 220; Introduction, 553; Discussion, 1,437.

Abbreviations: α MEM, alpha minimum essential medium; DIG, digoxigenin; DIV, days *in vitro*; GAPDH, glyceraldehydes-3-phosphate dehydrogenase; HKR, HEPES Krebs-Ringer; MCT, monocarboxylate transporters; DMEM, Dulbecco's modified eagle medium; μ CT, micro computed tomography; OVX, ovariectomy; ROS, reactive oxygen species.

ABSTRACT

We previously demonstrated that exogenous pyruvate has a protective action against cell death by hydrogen peroxide in cultured osteoblasts through a mechanism associated with its anti-oxidative property. In the present study, we have evaluated possible participation of monocarboxylate transporters (MCTs) responsible for the bi-directional membrane transport of pyruvate in the cytoprotective property in osteoblasts. Expression of MCT2 isoform was found in cultured rat calvarial osteoblasts and in osteoblasts located on mouse tibia at both mRNA and protein levels. The accumulation of [^{14}C]pyruvate occurred in a temperature- and pH-dependent manner in osteoblasts cultured for 7 days with high sensitivity to a specific MCT inhibitor, while pyruvate was released into extracellular spaces from cultured osteoblasts in a fashion sensitive to the MCT inhibitor. Transient overexpression of MCT2 isoform led to reduced vulnerability to the cytotoxicity of hydrogen peroxide with an increased activity of [^{14}C]pyruvate accumulation in murine osteoblastic MC3T3-E1 cells. Ovariectomy significantly decreased the content of pyruvate in femoral bone marrows in mice *in vivo*, while daily intraperitoneal administration of pyruvate at 0.25 g/kg significantly prevented alterations of several histomorphometric parameters as well as cancellous bone loss in femurs by ovariectomy on 28 days after the operation. These results suggest that MCTs may be functionally expressed by osteoblasts to play a pivotal role in mechanisms related to the cytoprotective property of pyruvate.

The view that pyruvate and other monocarboxylates such as lactate are transported into the cytoplasm across the plasma membrane by free diffusion and/or carriers including monocarboxylate transporters (MCTs) and Band3 is prevailing (Halestrap and Price, 1999; Rafiki et al., 2003). MCTs are divided into two types: one is H⁺-linked transporters and the other is Na⁺-linked transporters. The latter Na⁺-dependent MCTs are highly expressed on the luminal membrane of kidney and intestine with a role in the reabsorption of monocarboxylates such as lactate and pyruvate, in addition to ketone bodies, which are all essential for the body as energy resources (Halestrap, 1976). By contrast, the former H⁺-linked MCTs are transmembrane carriers that mediate the transport of monocarboxylates through pH and substrate concentration gradients (Halestrap and Price, 1999). MCTs have 14 family members (Halestrap and Price, 1999), including T-type amino acid transporter that carries aromatic amino acids (Rafiki et al., 2003; Halestrap, 1976). Of these different member proteins, however, only MCT1 to MCT4 isoforms are able to mediate the transport of pyruvate, lactate and other major monocarboxylates across plasma membranes (Halestrap and Meredith, 2004; Friesema et al., 2003; Kim et al., 2001).

In our previous study, pyruvate deficiency leads to severe cell death in both primary cultured rat calvarial osteoblasts and the clonal murine osteoblastic cell line MC3T3-E1 cells at a proliferative stage, but not those at differentiation and maturation stages, without significantly affecting the viability of rat costal chondrocytes and the murine stromal cell line ST2 cells (Hinoi et al., 2002). We have also demonstrated that exogenous pyruvate could have a protective action against cell death by hydrogen peroxide (H₂O₂) in cultured osteoblasts through a mechanism associated with its anti-oxidative property rather than an energy fuel (Moriguchi et al., 2006). In fact, evidence is accumulating for the cytoprotective properties of pyruvate against oxidative stress through direct scavenging of reactive oxygen species (ROS) including H₂O₂ in the literature. For example, pyruvate is shown to chemically

MOL #24398

react with H_2O_2 to yield carbon dioxide, water and acetic acid as follows: $\text{CH}_3\text{COCOO}^- + \text{H}_2\text{O}_2 \rightarrow \text{CH}_3\text{COO}^- + \text{CO}_2 + \text{H}_2\text{O}$, preventing the formation of hydroxyl radical ($\text{OH}\bullet$) from H_2O_2 (Holleman, 1904; Bunton, 1949). In cultured mouse striatal neurons, pyruvate is effective in strongly preventing the neurotoxicity of H_2O_2 extracellularly added and intracellularly formed from the quinone derivative menadione (Desagher et al., 1997), respectively. Similar cytoprotection by pyruvate is seen against apoptosis induced by H_2O_2 in the bovine pulmonary endothelium (Kang et al., 2001) and human endothelial cells (Lee et al., 2004), cell death after ischemic injury in cultured rat astrocytes (Sharma et al., 2003), neurotoxicity by 6-hydroxydopamine, 1-methyl-4-phenylpyridinium and H_2O_2 in murine brain neuroblastoma cells (Mazzio and Soliman, 2003) and zinc toxicity in cultured mouse cortical neurons *in vitro* and in rat hippocampus and cortex *in vivo* (Sheline et al., 2000; Lee et al., 2001). However, little attention has been paid to the possible involvement of the bi-directional transmembrane transport mediated by MCTs in the cytoprotective properties of pyruvate to date.

In the present study, therefore, we have attempted to demonstrate the possible functional expression of different MCT isoforms by osteoblastic cells in order to elucidate mechanisms underlying the protective property of pyruvate against the cytotoxicity of H_2O_2 using rat calvarial osteoblasts as well as murine osteoblastic MC3T3-E1 cells overexpressing a particular MCT isoform *in vitro*, in addition to ovariectomized mice *in vivo*.

Materials and Methods

Culture of Primary Osteoblasts. The protocol employed here meets the guideline of the Japanese Society for Pharmacology and was approved by the Committee for Ethical Use of Experimental Animals at Kanazawa University. All efforts were invariably made to minimize animal suffering, to reduce the number of animals used and to utilize alternatives to *in vivo* techniques. Osteoblasts were prepared from calvaria of 1- to 2-day-old Wistar rats by a sequential enzymatic digestion method as described previously (Hinoi et al., 2002). In brief, calvaria were gently digested at 37°C for 10 min five times with 0.1% collagenase and 0.25% trypsin, and the last three fractionated cells were collected altogether as the preparation for primary osteoblasts. Cells were plated at a density of 1×10^4 /cm² to appropriate dishes, and then cultured at 37°C for different periods up to 28 days *in vitro* (DIV) under 5% CO₂. Culture medium was alpha minimum essential medium (α MEM; Gibco, Gaithersburg, MD, USA) containing 10% FBS, 50 μ g/mL ascorbic acid and 5 mM sodium β -glycerophosphate. Medium was changed every 3 days. In some experiments, eutrophic α -MEM (1 mM pyruvate) was replaced with normally trophic Dulbecco's modified eagle medium (DMEM; no pyruvate) conditioned or not conditioned by rat costal chondrocytes cultured for different periods of 7 to 28 DIV, followed by determination of cell viability 12 h after the medium replacement unless otherwise indicated (Hinoi et al., 2002). Cell survival analysis was performed by Trypan blue staining method and cell counting kits (Dojindo, Osaka, Japan), respectively.

Culture of Primary Chondrocytes. Cartilages were isolated from adult female Wistar rat ribs, followed by incubation at 37°C for 10 min in Ca²⁺- and Mg²⁺-free PBS containing 0.1% EDTA and subsequent digestion with collagenase in DMEM at 37°C for 2.5 h. Cells were collected in DMEM containing 10 % FBS and antibiotics and then centrifuged

at 500 g for 5 min. The pellets were suspended in DMEM containing 10 % FBS. Cells were plated at a density of 4×10^4 cells/cm², followed by culture at 37°C under 5% CO₂ for an additional 6 DIV. Culture medium was exchanged to DMEM supplemented with 10% FBS and 50 µg/mL ascorbic acid for subsequent culture for different periods of up to 28 DIV. Medium was changed every 3 days. Conditioned medium was collected during the last 3 days before the routine medium change from chondrocytes cultured for a period of up to 28 DIV as needed.

RT-PCR Analysis. cDNA was synthesized with the oligo-dT primer and reverse transcriptase (Invitrogen, Carlsbad, CA, USA) from extracted total RNA. PCR amplification was performed using specific primers, and PCR products were subcloned into a TA cloning vector (Promega, Madison, WI, USA) for determination of DNA sequences by ABI Prism 310 Genetic Analyzer (Perkin-Elmer, Wellesley, MA, USA) using cycle sequencing kit (Amersham, Piscataway, NJ, USA). Quantitative analysis was done with primers for the housekeeping gene glyceraldehyde-3-phosphate dehydrogenase (GAPDH). PCR products were quantified by using a densitograph, followed by calculation of ratios of expression of mRNA for each gene over that for GAPDH.

Immunoblotting Analysis. Cultured osteoclasts were homogenized in 20 mM Tris-HCl buffer (pH 7.5) containing protease inhibitors, followed by centrifugation at 4°C for 30 min at 100,000 g as described elsewhere (Hinoi et al., 2003). Pellets thus obtained were dissolved in 10 mM Tris-HCl buffer containing 2% SDS and 5% 2-mercaptoethanol, followed by boiling for 10 min and subsequent loading of an aliquot (10 µg protein) for electrophoresis on a 7.5% SDS-polyacrylamide gel toward blotting to a polyvinylidene fluoride membrane. After blocking by 5% skim milk dissolved in 20 mM Tris -HCl buffer (pH 7.5) containing 137 mM NaCl and 0.05% Tween 20 (TBST), the membrane was incubated with one of antibodies against MCT2 and MCT3 (Chemicon, Temecula, CA, USA) adequately diluted

with TBST containing 1% skim milk, and then with the secondary antibody conjugated with horseradish peroxidase. Finally, the membrane was incubated with ECLTM detection reagent to detect immunoreactive proteins, followed by exposure to X-ray film for different periods to obtain films appropriate for subsequent quantitative densitometry.

Immunocytochemistry. Osteoblasts were washed twice with PBS, followed by fixation with 4% paraformaldehyde in PBS for 20 min at room temperature and subsequent blocking with 10% bovine serum albumin in PBS containing 1% Triton X-100. Cells were then reacted with an antibody against MCT2 adequately diluted for 2 h at room temperature. Cells were then reacted with the secondary antibody, an anti-rabbit IgG antibody conjugated with fluorescein for observation under a confocal laser-scanning microscope (LSM 510; Carl Zeiss, Jena, Germany).

***In Situ* Hybridization Analysis.** Tibiae were isolated from 1-day-old (P1) mice, followed by fixation with 10% formalin and subsequent decalcification with 20% EDTA for *in situ* hybridization as previously described (Wang et al., 2005). In brief, tibiae were dissected for frozen sections with a thickness of 5 μ m in a cryostat. Sections mounted on slide glasses were fixed with 4% paraformaldehyde, and successively treated with 0.2 M HCl and 10 μ g/mL Proteinase K. Sections were then subjected to acetylation in 0.1 M triethanolamine/0.25% acetic anhydride. After pre-hybridization, sections were covered with digoxigenin (DIG)-labeled cRNA probes at 65°C for 16 h. Sections were then washed, and treated with 4 μ g/mL RNase A. Sections were then incubated with anti-DIG-AP Fab fragments at 4°C for 16 h. After being washed, sections were treated with nitro blue tetrazolium chloride/5-bromo-4-chloro-3-indolyl phosphate for different periods.

Immunohistochemistry. Sections prepared from P1 mouse tibia were fixed with 4 % paraformaldehyde in PBS for 20 min, washed with PBS, treated with 0.3 % H₂O₂ in methanol for 30 min and washed with 70% ethanol for 5 min. After being washed with PBS,

MOL #24398

sections were subjected to blocking with PBS containing normal goat serum or BSA and 0.1% Triton X-100 at room temperature for 1 h. Sections were then reacted with an antibody against MCT2 isoform (1:200 dilution) diluted with the same blocking buffer at room temperature overnight, followed by reaction with a biotinylated anti-guinea-pig, anti-mouse or anti-rabbit IgG antibody at room temperature for 30 min and subsequent incubation with VECTASTAIN Elite ABC Reagent at room temperature for 1 h. Finally, immunostaining was done using 0.05% diaminobenzidine and 0.03% H₂O₂. Simultaneous experiments were invariably done in the absence of each primary antibody to confirm expression of the respective immunoreactive proteins.

Determination of [¹⁴C]Pyruvate Accumulation. Osteoblasts were cultured for an adequate period, followed by washing with HEPES Krebs-Ringer (HKR) (125 mM NaCl, 3.5 mM KCl, 1.5 mM CaCl₂, 1.2 mM MgSO₄, 1.25 mM KH₂PO₄, 25 mM NaHCO₃, 10 mM HEPES and 10 mM D-glucose, pH 7.4) buffer twice and subsequent incubation in HKR buffer at 37°C for 1 h in a 5% CO₂ incubator. Cells were then incubated with 1 to 10 μM [¹⁴C]pyruvate (23 mCi/mmol; Amersham, Piscataway, NJ, USA) at 2°C or 37°C for 1 to 60 min. Reaction was terminated by the careful aspiration of buffer, followed by gentle superficial rinsing with ice-cold HKR buffer containing 1 mM unlabeled pyruvate at 2°C 3 times to remove extracellular [¹⁴C]pyruvate and subsequent solubilization with 0.1 M NaOH for liquid scintillation spectrometry using 3 mL scintillation cocktail (clear sol I). Protein concentration was determined with a Bio-Rad Protein Assay Kit (Bio-Rad, Hercules, CA, USA).

Determination of Pyruvate Release. Culture medium was replaced with αMEM (pyruvate concentration = 1 mM) or DMEM (no pyruvate), and an aliquot of incubation medium was subsequently collected for reaction with 1 M perchloric acid at a volume ratio of 4:1. Following centrifugation at 20,000 g for 5 min, the supernatant was collected for

MOL #24398

subsequent neutralization with sodium hydroxide and stored at -80°C until use. Pyruvate was determined by the fluorometric method using NADH and lactate dehydrogenase. Samples were incubated with 100 mM NADH to make a final concentration of 2 mM, and then with 1.6 U/mL lactate dehydrogenase at a volume ratio of 1:1 for 5 min at 37°C . Pyruvate was measured in a fluorescence microplate reader (MPT-100F; Corona, Naka-Hitachi, Japan) with excitation at 340 nm and emission at 460 nm, respectively. In each experiment, pyruvate at known concentrations was determined in parallel as standards.

Transient Transfection. Mouse full-length coding region of MCT2 isoform was amplified by RT-PCR from mRNA prepared from the murine osteoblastic cell line MC3T3-E1 cells (RIKEN, Tsukuba, Ibaraki, Japan) using the following primers: 5'-GTTTCTTCCACTCTCAGGATGC-3' and 5'-GCAGGAGGAGGCAGGAGACCCGG-3'. The PCR-amplified DNA products were cloned into the pcDNA3.1 (Promega, Madison, WI, USA). MC3T3-E1 cells were cultured in α MEM supplemented with 10% FBS in a humidified 5% CO_2 incubator. MC3T3-E1 cells were seeded at 5×10^4 cells/cm² in 6 well plates. After 24 h, they were transiently transfected with pcDNA3.1 containing the full-length coding region of MCT2 isoform or with the empty vector using 2 μg of DNA and Lipofectamine and Plus reagent (Invitrogen, Carlsbad, CA, USA).

Ovariectomy (OVX) and Analysis of Skeletal Morphology. Eight-week-old female ddY mice were subjected to OVX or sham operation. Mice were killed by decapitation 28 days after OVX, followed by dissection of both femora and tibiae and subsequent removal of adhering muscles around the bone for fixation with 70% ethanol. Bone mineral density of different bones isolated from mice 28 days after operation was measured by single energy x-ray absorptiometry using a bone mineral analyzer (DCS-600R; Aloka Co., Tokyo, Japan). Animals were intraperitoneally injected with pyruvate at 0.25 g/kg once a day for consecutive

MOL #24398

28days as needed. Histomorphometric analysis was carried out using femur excised from mice 28 days after sham or OVX operation. For toluidine blue O staining, femur was fixed in 70 % ethanol, embedded in glycolmethacrylate and sectioned in 3 μ m thickness. The specimens were subjected to histomorphometric analysis under a light microscope with micrometer, using a semiautomatic image analyzing system (Osteoplan II; Carl Zeiss, Thornwood, NY, USA).

Data Analysis. Results are all expressed as the mean \pm S.E. and the statistical significance was determined by the two-tailed and unpaired Students' *t*-test or the one-way analysis of variance ANOVA with Bonferroni/Dunnett post hoc test.

Results

Effect of Pyruvate on Cell Death by Menadione and H₂O₂. In order to confirm the protective property of exogenous pyruvate, osteoblasts cultured for 3 or 7 DIV were exposed for 3 h to the quinone derivative menadione at concentrations of up to 50 μ M or H₂O₂ at concentrations of up to 1 mM in either the presence or absence pyruvate at 1 mM in DMEM. The exposure to menadione for 3 h led to a significant decrease in the cell viability in a concentration-dependent manner at concentrations of above 1 μ M in osteoblasts cultured for 3 DIV (Fig. 1A, upper panel) and at concentrations of over 30 μ M in cells cultured for 7 DIV (Fig. 1A, lower panel), respectively. Similarly, H₂O₂ was more effective in significantly inhibiting the viability in cells cultured for 3 DIV (Fig. 1B, upper panel) than in those for 7 DIV (Fig. 1B, lower panel) in a concentration range of 10 μ M to 1 mM. However, the addition of pyruvate at 1 mM invariably prevented the loss of cell viability induced by both menadione and H₂O₂ at all concentrations examined irrespective of the culture duration.

Expression Profiles of MCTs. In rat calvarial osteoblasts cultured for 3 or 7 DIV, mRNA was constitutively expressed for several MCT isoforms responsible for the active transport of pyruvate across plasma membranes irrespective of the cell maturity (Fig. 2A). These included MCT1, MCT2 and MCT4 isoforms, while MCT3 mRNA was not detected in immature osteoblasts cultured for 3 DIV. Sequencing analysis on amplified PCR products clearly confirmed the identity of mRNA for all MCT isoforms examined (data not shown). In osteoblasts cultured for 3 to 28 DIV, moreover, constitutive expression was detected for MCT2, but not for MCT3, isoform at the corresponding molecular weight positions identical to those from rat whole brain on the gel when determined by Western blotting (Fig. 2B). Corresponding protein for MCT2 isoform was also detected in osteoblasts cultured for 7 DIV using the anti-MCT2 antibody (Fig. 2C). For the confirmation of expression of particular

MOL #24398

isoforms of MCTs by osteoblasts in bone, tibiae were isolated from newborn P1 mice, followed by dissection of frozen sections for subsequent *in situ* hybridization and immunohistochemistry analyses. *In situ* hybridization evaluation clearly demonstrated the expression of MCT2 isoform by osteoblasts when the antisense RNA probe was used (Fig. 2D, upper left and middle panels), while no signal was found for MCT2 isoform with the sense probe (Fig. 2D, upper right panel). Immunohistochemical analysis revealed a similar expression profile with immunoreactive MCT2 on osteoblasts in tibial sections (Fig. 2D, lower left and middle panels). In sections not treated with a primary antibody, no marked immunoreactivity was detected in any bone tissues (Fig. 2D, lower right panel). Although mRNA expression of MCT3 isoform was detected on osteoblasts in bone (Fig. 2E lower panels), by contrast, no apparent signal of MCT1 isoform was found in bone isolated from tibia by the specific anti-sense RNA probe (Fig. 2E upper panel). Therefore, subsequent experiments focused on evaluation of the functionality of MCTs required for the membrane transport of pyruvate.

[¹⁴C]Pyruvate Accumulation. Cultured osteoblasts were incubated with 10 μM [¹⁴C]pyruvate in HKR buffer at 2°C or 37°C for different periods up to 90 min, followed by rapid aspiration of buffer and subsequent rinsing with ice-cold buffer containing unlabeled pyruvate at 1 mM to remove extracellularly located [¹⁴C]pyruvate. Under these experimental conditions, [¹⁴C]pyruvate incorporated was not markedly affected by the later addition of 1 mM unlabeled pyruvate for rinsing in cultured osteoblasts (data not shown). Although the accumulation of [¹⁴C]pyruvate was increased in proportion to incubation periods in a temperature-dependent manner with a plateau before 40 min in osteoblasts cultured for 7 DIV (Fig. 3A, right panel), the temperature-dependent [¹⁴C]pyruvate incorporation was not detected in osteoblasts cultured for 3 DIV at any time windows examined (Fig. 3A, left panel). The temperature-dependent accumulation was increased at 37°C with increasing

MOL #24398

concentrations of [^{14}C]pyruvate at 1 to 600 μM , followed by a saturable profile at a concentration above 400 μM (Fig. 3B). Woolf-Hanes plot analysis revealed that [^{14}C]pyruvate accumulation consisted of a single component with a K_m value of 558 ± 83 μM and a V_{max} value of 6596 ± 748 pmol/min/mg protein, respectively, at the substrate concentration range employed. Cells were incubated with several MCT inhibitors at a concentration range of 10 nM to 1 mM for 20 min at 37°C . Of the six different inhibitors tested, UK5099 ($\text{IC}_{50}=664\pm 100$ nM) was most potent in inhibiting [^{14}C]pyruvate accumulation with progressively less potent inhibition by quercetin ($\text{IC}_{50}=15.9\pm 6.1$ μM), α -cyano-3-hydroxycinnamate ($\text{IC}_{50}=103\pm 48$ μM), 3-isobutyl-1-methylxanthine ($\text{IC}_{50}=127\pm 31$ μM), 4,4'-diisothiocyanostilbene-2,2'-disulfonate ($\text{IC}_{50}=400\pm 28$ μM) and L-lactate ($\text{IC}_{50}=905\pm 34$ μM) (Fig. 3C). As shown in Fig. 3D, moreover, [^{14}C]pyruvate accumulation was decreased in proportion to increasing pHs at a range of 5.5 to 8.0 in osteoblasts cultured for 7 DIV.

Pyruvate Release and Cell Viability. To demonstrate the bi-directional pyruvate membrane transport through MCTs, osteoblasts cultured for 3 or 7 DIV were incubated in DMEM (no pyruvate) or α MEM (1 mM pyruvate) for different periods of up to 48 h in either the presence or absence of the specific MCT inhibitor UK5099, followed by determination of pyruvate released into culture medium during incubation. The release of pyruvate was almost linearly increased with incubation time up to 30 h and reached a plateau within 48 h when culture medium was replaced with DMEM from α MEM in osteoblasts cultured for 7 DIV, while no marked release of pyruvate was seen at any time after medium replacement with DMEM in osteoblasts cultured for 3 DIV (Fig. 4A). In osteoblasts cultured for 7 DIV, UK5099 significantly inhibited the release of pyruvate at 500 μM into medium during incubation for a period up to 48 h after medium replacement with DMEM, and completely blocked the release at 1 mM for up to 24 h (Fig. 4B).

We next investigated the effect of the MCT inhibitor UK5099 on cell viability. Osteoblasts cultured for 7 DIV were exposed to UK5099 at 500 μ M in either the presence or absence of pyruvate at 1 mM for 24 h or 48 h in DMEM, followed by determination of cell viability by Trypan blue staining. The addition of UK5099 significantly increased the number of osteoblasts positive to Trypan blue staining, while simultaneous treatment with pyruvate at 1 mM significantly but partially decreased the number of Trypan blue-positive cells in osteoblasts exposed to UK5099 for 24 h (Fig. 4C) or 48 h (Fig. 4D).

Pyruvate in Chondrocytes. In order to evaluate the possible release of pyruvate from other cells adjacent to osteoblasts, an attempt was made to determine whether chondrocytes are able to release pyruvate through MCTs for the protection of osteoblasts against the cytotoxicity after medium replacement. For this purpose, chondrocytes were prepared from the adult rat costal cartilage, followed by the cultivation in DMEM (no pyruvate) for 7 to 28 DIV and subsequent collection of conditioned medium on different days. In costal chondrocytes cultured for 7 or 21 DIV, mRNA expression was seen for MCT1, MCT2 and MCT4 isoforms, but not for MCT3 isoform, irrespective of the cell maturity (Fig. 5A). Pyruvate was detected at similar concentrations in culture medium collected during the last 3 days from chondrocytes cultured for a period of 7 to 28 DIV, but not detectable in the culture medium (Fig. 5B). The chondral conditioned medium was then used for the replacement from α MEM in immature osteoblasts cultured for 3 DIV. The replacement with such chondral conditioned DMEM led to drastic and similarly effective protection of immature osteoblasts cultured for 3 DIV against cell death when determined 12 h after the medium replacement from α MEM (1 mM pyruvate) independent of the duration of chondrocyte culture (Fig. 5C).

Effect of MCT2 Overexpression on Cell Viability. To assess the role of MCT2 isoform in osteoblastic cell death by H₂O₂, murine osteoblastic cell line MC3T3-E1 cells were

transiently transfected with pcDNA3.1 containing the full-length coding region of MCT2 isoform (MC3T3-E1-MCT2) or with the empty vector (MC3T3-E1-EV). MC3T3-E1-MCT2 cells displayed markedly elevated expression of MCT2 isoform compared to MC3T3-E1-EV cells on semi-quantitative RT-PCR for their corresponding mRNA (Fig. 6A). In addition to upregulation of MCT2 mRNA expression, transient overexpression of MCT2 more than tripled [¹⁴C]pyruvate accumulation in MC3T3-E1 cells (Fig. 6B). Both MC3T3-E1-EV and MC3T3-E1-MCT2 cells were exposed to H₂O₂ for 3 h at a concentration range of up to 500 μM 48 h after transfection, followed by determination of cell viability. Cell viability was significantly decreased in the presence of H₂O₂ in a concentration-dependent manner at concentrations used in MC3T3-E1-EV cells, while transient overexpression of MCT2 isoform led to less vulnerability to H₂O₂ than that found in MC3T3-E1-EV cells at the concentration range of 200 to 400 μM (Fig. 6C). Even in MC3T3-E1-MCT2 cells, however, more than 60% of cells were dead after the exposure to H₂O₂ at 500 μM for 3 h.

Effect of Pyruvate on OVX-induced Bone Loss. To examine whether pyruvate also prevents bone loss *in vivo*, we next conducted OVX in mice for subsequent determination of the bone mineral density in addition to different histomorphometric analyses. No significant change was seen in body weight at any days after OVX up to 28 days irrespective of pyruvate administration (data not shown), whereas OVX significantly decreased the endogenous level of pyruvate in femoral bone marrows by about 30% when compared with that in sham-operated mice on 28 days after operation (Fig. 7A). Ovariectomy drastically decreased uterine weight on 28 days after operation, but the daily intraperitoneal administration of pyruvate did not significantly affect the OVX-induced loss of uterine weight (Fig. 7B). Ovariectomy also induced a significant reduction of the bone mineral density in total tibia, total femur and distal femur when determined by single-energy X-ray absorptiometry on 28 days later, while the daily administration of pyruvate significantly prevented the reduction of

bone mineral density in total tibia, total femur and distal femur (Fig. 7C).

Ovariectomy also led to severe bone loss in cancellous bone (Fig. 8A, left pictures) but not in cortical bone (Fig. 8A, right pictures) when determined by micro-computed tomography (μ CT) analysis, moreover, whereas daily intraperitoneal administration of pyruvate prevented the OVX-induced bone loss seen in cancellous bone (Fig. 8A, bottom left picture). Similar protection profiles were confirmed in animals injected with pyruvate on toluidine blue staining (Fig. 8B). Histomorphometric analysis revealed that OVX significantly decreased several parameters including BV/TV (bone volume/tissue volume), Tb.Th (trabecular thickness) and Tb.N (trabecular number), in addition to increasing the parameter Tb.Sp (trabecular separation) (Fig. 8C). Daily administration of pyruvate significantly prevented these alterations by OVX of different histomorphometric parameters.

Discussion

The essential importance of the present findings is that pyruvate significantly prevented cell death by the quinone derivative menadione responsible for the intracellular generation of H₂O₂ (Desagher et al., 1997), in association with the functional expression of a particular MCT isoform, irrespective of the cellular maturity in cultured rat calvarial osteoblasts. Pyruvate also prevented cell death by extracellularly added H₂O₂ in primary rat osteoblasts, moreover, while transient overexpression of MCT2 isoform significantly attenuated the cytotoxicity seen after the brief exposure to H₂O₂ with concomitant acceleration of [¹⁴C]pyruvate accumulation rates in the murine osteoblastic cell line MC3T3-E1 cells. To our knowledge, this indicates for the first time the functional expression of MCT2 isoform required for the bi-directional transmembrane transport of pyruvate with cytoprotective properties against oxidative stress in osteoblasts. Several previous studies including ours have already demonstrated the protection by exogenous pyruvate against cell death induced by ROS in a variety of cells, whereas no direct evidence for a pivotal role of MCTs in mechanisms underlying the cytoprotective property in osteoblasts is available in the literature to date. The *in vitro* data cited in this study thus give rise to an idea that exogenous pyruvate could protect osteoblasts against the cytotoxicity of ROS after the incorporation mediated by MCTs expressed at cell surfaces into the cytoplasm for a subsequent direct chemical reaction with H₂O₂ to yield acetate, carbon dioxide and water as described above. However, extracellular direct interaction would also at least in part participate in the cytoprotection by pyruvate. From this point of view, it should be noted that immature osteoblasts cultured for 3 DIV exhibited both mRNA expression of different MCT isoforms and acquired resistance to the cytotoxicity of menadione in the presence of exogenous pyruvate, in spite of the absence of temperature-dependent [¹⁴C]pyruvate accumulation. In

this situation, extracellular pyruvate should enter the cytoplasm to prevent the cytotoxicity of intracellular H₂O₂ generated from menadione in immature cultured osteoblasts. Although temperature-independent [¹⁴C]pyruvate accumulation may play a role in the mechanism underlying the cytoprotection by extracellular pyruvate, the evaluation of its physiological and pathological significance seems to be beyond the scope of the present study.

Moreover, the daily administration of pyruvate significantly prevented decreases in both bone mineral density on single-energy X-ray absorptiometry and trabecular bone on μ CT in tibia and femur, in addition to alterations of different histomorphometric parameters, in ovariectomized mice *in vivo*. There is increasing evidence suggesting a crucial role of free oxygen radicals in the pathogenesis of postmenopausal osteoporosis in the literature. A close negative correlation is seen between oxidative stress (antioxidant levels) and bone mineral density in women (Basu et al., 2001; Maggio et al., 2002), for example, while H₂O₂ is suggested to be a ROS responsible for the bone loss in estrogen deficiency (Lean et al., 2005). In addition to postmenopausal osteoporosis, increased oxidative stress is supposed to play a role in mechanisms underlying osteopenia associated with other risk factors. These include diabetes mellitus (Christensen and Svendsen, 1999), atherosclerosis (Hamerman, 2005), smoking (Law and Hackshaw, 1997) and hypertension (Cappuccio et al., 1999). The *in vivo* data shown in this investigation therefore give support to the proposal that pyruvate could be useful for the therapy and/or the prophylaxis of a variety of the aforementioned bone diseases relevant to the cytotoxicity of oxidative stress.

Although pyruvate may be released from relatively mature, but not immature, osteoblasts in a manner sensitive to the MCT inhibitor, the exact origin as well as source of pyruvate available for the cytoprotection in osteoblasts *in situ* is not fully clarified so far. On the analogy to the present study on the functional expression of particular MCT isoforms by osteoblasts and chondrocytes, we have also investigated the expression profile of different

MOL #24398

MCT isoforms by mouse osteoclasts differentiated from bone marrow hematopoietic precursors. Irrespective of the detection of mRNA expression of MCT1, MCT2 and MCT4, but not for MCT3, isoforms, however, no marked accumulation of [¹⁴C]pyruvate was seen in cultured mouse osteoclasts at any developmental stages (preliminary data). This means that pyruvate could be released from chondrocytes adjacent to osteoblasts in bone, but not from osteoclasts, through the retrograde transport mediated by MCTs to protect osteoblastic cells against oxidative stress, in addition to the MCT-mediated release from mature osteoblasts *per se* as summarized in Fig. 9. In the present study, in fact, cell death after the medium replacement was significantly prevented following the addition of conditioned medium prepared from rat costal chondrocytes cultured for different periods with pyruvate at an effective concentration in immature osteoblasts. In contrast to osteoblasts, however, chondrocytes seem to similarly release pyruvate irrespective of the cell maturity.

In contrast to the efficient inhibition of [¹⁴C]pyruvate accumulation, a considerably high concentration was required for UK5099 to inhibit the gradual release of endogenous pyruvate after the medium replacement from α MEM (1 mM pyruvate) with DMEM (no pyruvate) in matured osteoblasts cultured for 7 days. Therefore, the possibility that UK5099 would inhibit the slow efflux of endogenous pyruvate through a mechanism related to the inhibition of transporters other than MCTs and/or the intracellular pyruvate synthesis during such a long incubation period is not ruled out. An attempt to evaluate the possible efflux of preloaded [¹⁴C]pyruvate within a short period of incubation from cultured osteoblasts, however, was unsuccessful in our preliminary experiments. Preloaded [¹⁴C]pyruvate was not released to a detectable level within 10 min in a temperature-dependent manner with sensitivity to UK5099 (data not shown). There is no evidence that [¹⁴C]pyruvate is incorporated into the compartment accessible by endogenous pyruvate and releasable after the medium replacement in the cytoplasm. Extracellular pyruvate could be accumulated into an

intracellular compartment unavailable for the immediate efflux through a particular MCT isoform expressed on plasma membranes in cultured osteoblasts. In this investigation, in fact, endogenous pyruvate was not released to a detectable amount from matured osteoblasts within 1 h after the medium replacement. Endogenous pyruvate would be gradually released to compensate the long-term absence of pyruvate from extracellular environments in a particular situation. One possible but hitherto unidentified speculation is that UK5099 should be at first incorporated across plasma membranes into the cytoplasm to gain access to an intracellular site responsible for the efflux through the retrograde operation of bi-directional transporters such as MCTs, in contrast to the inhibition of the anterograde operation through an extracellular site required for the influx. If this is really the case, the inhibition by UK5099 should be more efficient in [¹⁴C]pyruvate accumulation than the gradual efflux of endogenous pyruvate after medium replacement as seen in this study. Accordingly, pyruvate may play a pivotal role in the mechanisms underlying cell survival and maturation through the bi-directional transport mediated by MCTs across plasma membranes in immature osteoblasts.

Ovariectomy is shown to significantly decrease the endogenous level of reduced glutathione in addition to the activity of glutathione reductase in bone marrows (Lean et al., 2003). The administration of antioxidants such as N-acetyl cysteine and ascorbic acid, increases glutathione levels with concomitant prevention of the OVX-induced bone loss, while L-buthionine-(S,R)-sulphoximine, a specific inhibitor of glutathione synthesis, causes substantial bone loss (Lean et al., 2003). In addition, OVX-induced bone loss is indeed prevented by the administration of pegylated catalase, suggesting the possible involvement of H₂O₂ in OVX-induced bone loss (Lean et al., 2005). From the present findings that OVX markedly decreased the level of pyruvate in bone marrows in addition to decreasing bone mineral density, it is conceivable that pyruvate would be a candidate for the endogenous

MOL #24398

antioxidants enriched in bone marrows for the prevention of trabecular bone loss after the loading of different oxidative stressors including ROS. The possibility that pyruvate would be also preventive against bone loss induced by a prolonged loading of ROS signals such as ageing and inflammation, thus, is not ruled out so far.

It thus appears that pyruvate may be protective against bone loss induced by different oxidative stressors through a direct scavenging action after the incorporation mediated by MCTs into the cytoplasm. In physiological situations, pyruvate could be released by MCTs to scavenge extracellular ROS toxic to cells following the biosynthesis from glucose during glycolysis, in addition to scavenging intracellular ROS. Both the activity and the vector of bi-directional MCTs expressed at cell surfaces would therefore be a crucial determinant of cellular viability through modulation of the endogenous level of intracellular pyruvate that plays a dual role as an antioxidant and an energy fuel in osteoblasts. Therefore, particular MCT isoforms would be a novel target with a great benefit for the discovery and development of innovative strategies useful for the therapy and treatment of a variety of diseases associated with cellular damages by ROS such as osteoporosis.

Acknowledgments

The authors are grateful to Pfizer Limited (Sandwich, Kent, UK) for a kind gift of UK5099.

References

- Basu S, Michaelsson K, Olofsson H, Johansson S and Melhus H (2001) Association between oxidative stress and bone mineral density. *Biochem Biophys Res Commun* **288**:275-279.
- Bunton CA (1949) Oxidation of α -diketones and α -keto-acids by hydrogen peroxide. *Nature* **163**:444.
- Cappuccio FP, Meilahn E, Zmuda JM and Cauley JA (1999) High blood pressure and bone-mineral loss in elderly white women: a prospective study. Study of osteoporotic fractures research group. *Lancet* **354**:971-975.
- Christensen JO and Svendsen OL (1999) Bone mineral in pre- and postmenopausal women with insulin-dependent and non-insulin-dependent diabetes mellitus. *Osteoporos Int* **10**:307-311.
- Desagher S, Glowinski J and Premont J (1997) Pyruvate protects neurons against hydrogen peroxide-induced toxicity. *J Neurosci* **17**:9060-9067.
- Friesema EC, Ganguly S, Abdalla A, Manning Fox JE, Halestrap AP and Visser TJ (2003) Identification of monocarboxylate transporter 8 as a specific thyroid hormone transporter. *J Biol Chem* **278**:40128-40135.
- Halestrap AP (1976) Transport of pyruvate and lactate into human erythrocytes. Evidence for the involvement of the chloride carrier and a chloride-independent carrier. *Biochem J* **156**:181-183.
- Halestrap AP and Meredith D (2004) The SLC16 gene family-from monocarboxylate transporters (MCTs) to aromatic amino acid transporters and beyond. *Pflugers Arch* **447**:619-628.
- Halestrap AP and Price NT (1999) The proton-linked monocarboxylate transporter (MCT) family: structure, function and regulation. *Biochem J* **343**:281-299.

- Hamerman D (2005) Osteoporosis and atherosclerosis: biological linkages and the emergence of dual-purpose therapies. *QJM* **98**:467-484.
- Hinoi E, Fujimori S, Takemori A and Yoneda Y (2002) Cell death by pyruvate deficiency in proliferative cultured calvarial osteoblasts. *Biochem Biophys Res Commun* **294**:1177-1183.
- Hinoi E, Fujimori S and Yoneda Y (2003) Modulation of cellular differentiation by N-methyl-D-aspartate receptors in osteoblasts. *FASEB J* **17**:1532-1534.
- Holleman AF (1904) Notice sur l'action de l'eau oxygénée sur les acides α -cétoniques et sur les dicétones 1.2. *Rec Trav Chim Pays-Bas Belg* **23**:169-172.
- Kang YH, Chung SJ, Kang IJ, Park JH and Bunger R (2001) Intramitochondrial pyruvate attenuates hydrogen peroxide-induced apoptosis in bovine pulmonary artery endothelium. *Mol Cell Biochem* **216**:37-46.
- Kim DK, Kanai Y, Chairoungdua A, Matsuo H, Cha SH and Endou H (2001) Expression cloning of a Na⁺-independent aromatic amino acid transporter with structural similarity to H⁺/monocarboxylate transporters. *J Biol Chem* **276**:17221-17228.
- Law MR and Hackshaw AK (1997) A meta-analysis of cigarette smoking, bone mineral density and risk of hip fracture: recognition of a major effect. *BMJ* **315**:841-846.
- Lean JM, Davies JT, Fuller K, Jagger CJ, Kirstein B, Partington GA, Urry ZL and Chambers TJ (2003) A crucial role for thiol antioxidants in estrogen-deficiency bone loss. *J Clin Invest* **112**:915-923.
- Lean JM, Jagger CJ, Kirstein B, Fuller K and Chambers TJ (2005) Hydrogen peroxide is essential for estrogen-deficiency bone loss and osteoclast formation. *Endocrinology* **146**:728-735.
- Lee JY, Kim YH and Koh JY (2001) Protection by pyruvate against transient forebrain ischemia in rats. *J Neurosci* **21**:RC171.

- Lee YJ, Kang IJ, Bungler R and Kang YH (2004) Enhanced survival effect of pyruvate correlates MAPK and NF-kappaB activation in hydrogen peroxide-treated human endothelial cells. *J Appl Physiol* **96**:793-801.
- Maggio D, Barabani M, Pierandrei M, Macchiarulo MC, Cecchetti R, Pedrazzoni M, Senin U and Cherubini A (2002) Antioxidants and bone turnover in involutional osteoporosis. *J Endocrinol Invest* **25**:101-102.
- Mazzio EA and Soliman KF (2003) Cytoprotection of pyruvic acid and reduced beta-nicotinamide adenine dinucleotide against hydrogen peroxide toxicity in neuroblastoma cells. *Neurochem Res* **28**:733-741.
- Moriguchi N, Hinoi E, Tsuchihashi Y, Fujimori S, Iemata M, Takarada T and Yoneda Y (2006) Cytoprotection by pyruvate through an anti-oxidative mechanism in cultured rat calvarial osteoblasts. *Histol Histopathol* **21**:969-977.
- Rafiki A, Boulland JL, Halestrap AP, Ottersen OP and Bergersen L (2003) Highly differential expression of the monocarboxylate transporters MCT2 and MCT4 in the developing rat brain. *Neuroscience* **122**:677-688.
- Sharma P, Karian J, Sharma S, Kiu S and Monaghan PD (2003) Pyruvate ameliorates post ischemic injury of rat astrocytes and protects them against PARP mediated cell death. *Brain Res* **992**:104-113.
- Sheline CT, Behrens MM and Choi DW (2000) Zinc-induced cortical neuronal death: contribution of energy failure attributable to loss of NAD(+) and inhibition of glycolysis. *J Neurosci* **20**:3139-3146.
- Wang L, Hinoi E, Takemori A, Takarada T and Yoneda Y (2005) Abolition of chondral mineralization by group III metabotropic glutamate receptors expressed in rodent cartilage. *Br J Pharmacol* **146**:732-743.

This work was supported in part by Grants-in-Aids for Scientific Research to E.H., T.T. and Y.Y. from the Ministry of Education, Culture, Sports, Science and Technology, Japan.

Present address of Dr. Wang: Department of Biochemistry, Osaka University Graduate School of Dentistry, 1-8 Yamadaoka, Suita, Osaka 565-0871, Japan

Figure Legends

Fig. 1. Effect of pyruvate on menadione- and H₂O₂-induced cell death in cultured osteoblasts. Osteoblasts cultured for 3 or 7 DIV were exposed to (A) menadione at a concentration range of 1 to 50 μ M or (B) H₂O₂ at a concentration range of 10 μ M to 1 mM for 3 h in either the presence or absence of pyruvate at 1 mM, followed by determination of cell viability. Values are the mean \pm S.E. from 6 to 8 different experiments. *P<0.05, **P<0.01, significantly different from each control value obtained in cells not exposed to menadione or H₂O₂. #P<0.05, ##P<0.01, significantly different from the value obtained in cells exposed to menadione or H₂O₂ in the absence of pyruvate.

Fig. 2. Expression profiles of MCTs in bone. (A) Primary osteoblasts were cultured in α MEM for 3 or 7 DIV in the presence of 50 μ g/mL ascorbic acid and 5 mM β -glycerophosphate, followed by isolation of mRNA and subsequent RT-PCR using respective primers specific for MCT1 to MCT4 isoforms. (B) Osteoblasts were cultured for 3 to 28 DIV, followed by homogenization and subsequent centrifugation at 100,000g for immunoblotting analysis using antibodies against MCT2 and MCT3 isoforms. Rat whole brain (WB) was used as a positive control. (C) Osteoblasts were cultured for 7 DIV and fixed with 4% paraformaldehyde for subsequent immunocytochemical analysis using an antibody against MCT2 isoform. Tibiae isolated from mice at postnatal 1 day (P1) were fixed with formalin, followed by dissection of frozen sections and subsequent *in situ* hybridization analysis using antisense and sense probes for MCT2 (D), MCT1 (E) and MCT3 (E) isoforms. Tibial sections were also subjected to immunohistochemical analysis using an antibody against MCT2 (D). Typical micrographic pictures are shown in the figure, while similar results were invariably obtained in at least 3 independent determinations.

Fig. 3. [^{14}C]Pyruvate accumulation in cultured osteoblasts. (A) Osteoblasts cultured for 3 or 7 DIV were incubated with $10\ \mu\text{M}$ [^{14}C]pyruvate at 2 or 37°C for different periods of up to 90 min in HKR buffer, followed by aspiration of buffer and subsequent rinsing with buffer containing unlabeled pyruvate at 1 mM. (B) Osteoblasts were cultured for 7 DIV, followed by incubation with [^{14}C]pyruvate at different concentrations from 1 to $600\ \mu\text{M}$ for 20 min at 37°C for determination of saturation isotherms. (C) Osteoblasts cultured for 7 DIV were incubated with [^{14}C]pyruvate at 37°C for 20 min in HKR buffer containing 6 different MCT inhibitors at a concentration range of 10 nM to 1 mM. (D) Osteoblasts cultured for 7 DIV were incubated with [^{14}C]pyruvate at 37°C for 20 min at a pH range from 5.5 to 8.0. Values are the mean \pm S.E. from different experiments shown in the figures. Abbreviations: CHCA, α -cyano-3-hydroxycinnamate, DIDS, 4,4'-diisothiocyanostilbene-2,2'-disulfonate; IBMX, 3-isobutyl-1-methylxanthine.

Fig. 4. Pyruvate release in cultured osteoblasts. (A) Osteoblasts were cultured in αMEM (1 mM pyruvate) for 3 or 7 DIV, followed by medium replacement from αMEM with αMEM or DMEM (no pyruvate) and subsequent further cultivation for different periods up to 48 h. (B) Osteoblasts were cultured in αMEM for 7 DIV, followed by medium replacement from αMEM with DMEM and subsequent further cultivation for different periods up to 48 h in either the presence or absence of UK5099 at $500\ \mu\text{M}$ or 1 mM. An aliquot of incubation medium was subjected to determination of pyruvate by the fluorometric method using NADH and lactate dehydrogenase. Osteoblasts cultured for 7 DIV were exposed to $500\ \mu\text{M}$ UK5099 in DMEM for 24 h (C) or 48 h (D) in either the presence or absence of pyruvate (Pyr) at 1 mM, followed by determination of cell viability. Values are the mean \pm S.E. from different experiments shown in the figures. ** $P < 0.01$, significantly different from the value obtained in

cells cultured in the absence of UK5099. [#]P<0.05, significantly different from the value obtained in cells cultured with UK5099 in the absence of added pyruvate.

Fig. 5. Cytoprotection by conditioned medium of chondrocytes. (A) Rat costal chondrocytes were cultured in DMEM (no pyruvate) for a period of 7 to 28 DIV, followed by isolation of mRNA and subsequent RT-PCR using respective primers specific for MCT1 to MCT4 isoforms. (B) Chondrocytes were cultured in DMEM for a period of 7 to 28 DIV, followed by collection of culture medium and subsequent determination of pyruvate. (C) Osteoblasts cultured for 3 DIV were subjected to medium replacement from α MEM (1 mM pyruvate) to DMEM (no pyruvate) conditioned or not conditioned by chondrocytes cultured for 7 to 28 DIV, followed by further cultivation for an additional 12 h and subsequent determination of cell viability. Values are the mean \pm S.E. in 6 independent measurements. **P<0.01, significantly different from the control value obtained in cells cultured in α MEM. ^{##}P<0.01, significantly different from the value obtained in cells cultured in the absence of conditioned medium.

Fig. 6. Effect of MCT2 overexpression on H₂O₂-induced cell death in MC3T3-E1 cells. Osteoblastic MC3T3-E1 cells were transiently transfected with MCT2 expression vector or empty vector (EV), followed by determination of expression levels of MCT2 by (A) semi-quantitative RT-PCR and (B) [¹⁴C]pyruvate accumulation activity. **P<0.01, significantly different from each control value obtained in cells transfected with EV alone. Both MC3T3-E1-MCT2 and MC3T3-E1-EV cells were exposed to H₂O₂ at a concentration of up to 500 μ M for 3 h, followed by determination of cell viability. Values are the mean \pm S.E. from different experiments shown in the figures. [#]P<0.05, ^{##}P<0.01, significantly different from each control value obtained in cells with EV.

Fig. 7. Effect of pyruvate administration on bone mineral density. Eight-week-old female ddY mice were subjected to OVX or sham operation, followed by determination of (A) pyruvate contents in femoral bone marrows and (B) uterine weight on 28 days after operation. (C) Animals were also given with daily intraperitoneal administration of pyruvate (Pyr) at 0.25 g/kg for consecutive 28 days, followed by measurement of bone mineral density in both tibia and femur on single-energy X-ray absorptiometry. Values are the mean±S.E. from different experiments shown in the figures. *P<0.05, **P<0.01, significantly different from each control value obtained in sham-operated mice. ^{##}P<0.01, significantly different from the value obtained in OVX mice.

Fig. 8. Micro-CT analysis and histomorphometric analysis. Eight-week-old female ddY mice were subjected to OVX or sham operation, followed by daily intraperitoneal administration of saline or pyruvate (Pyr) at 0.25 g/kg for 28 days and subsequent μ CT analysis (A), toluidine blue staining (B) and histomorphometric analysis (C). Values are the mean±S.E. from 3 to 4 different experiments. *P<0.05, **P<0.01, significantly different from each control value obtained in sham-operated mice. [#]P<0.05, significantly different from the value obtained in OVX mice. Abbreviations used: BV/TV, bone volume/tissue volume; Pyr, pyruvate; Tb.N, trabecular number; Tb.Sp, trabecular separation; Tb.Th, trabecular thickness.

Fig. 9. Schematic model of pyruvate action in bone. Particular functional MCTs are identified in matured osteoblasts as well as in chondrocytes, but not in immature osteoblasts with high vulnerability to ROS. Pyruvate could be released from both matured osteoblasts and chondrocytes through particular MCT isoforms to protect immature osteoblasts against the cytotoxicity of ROS.

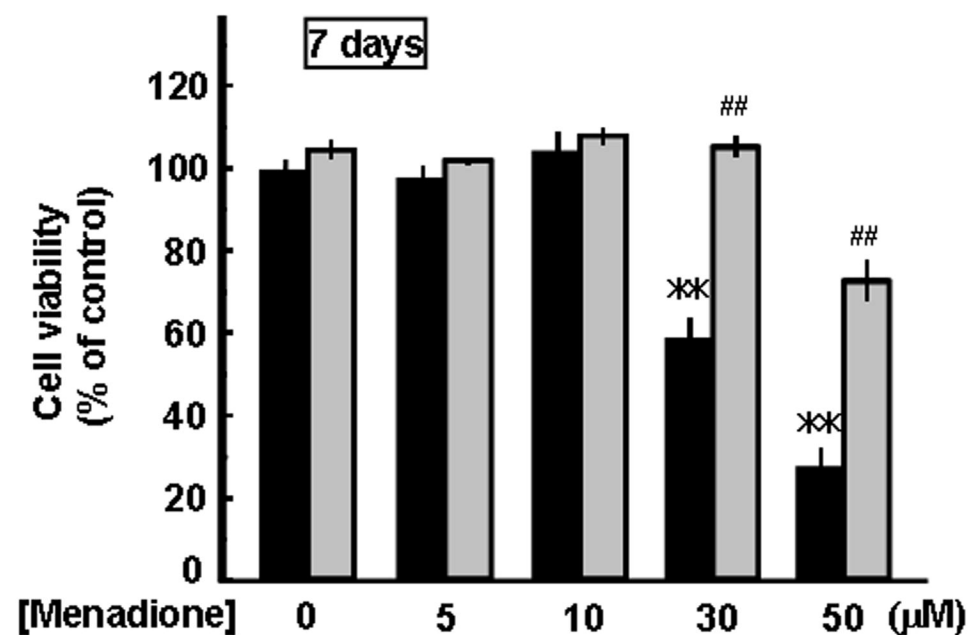
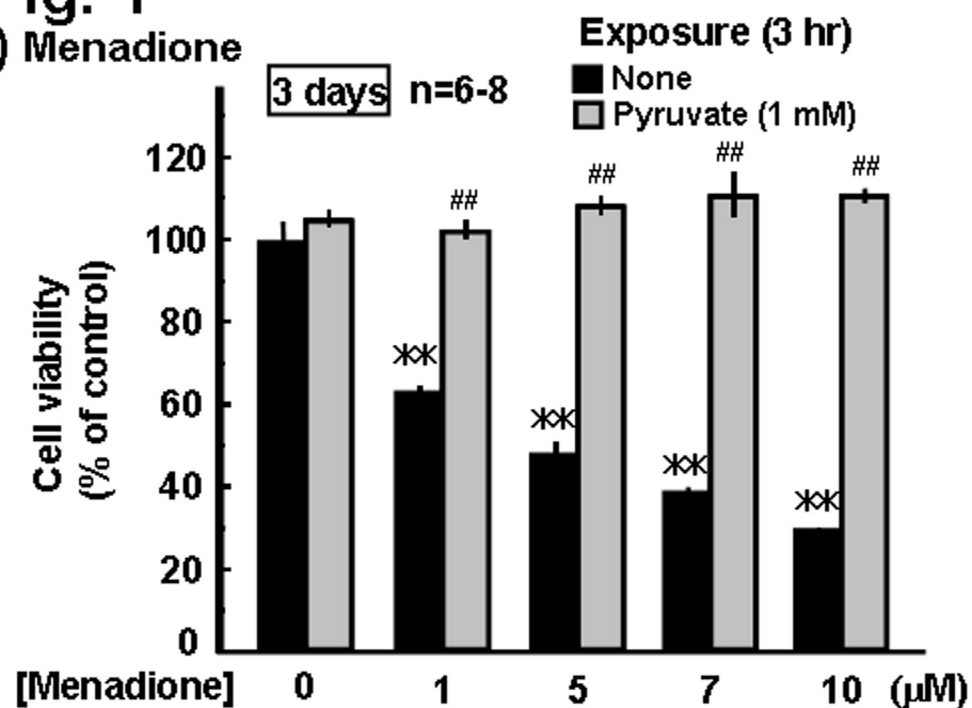
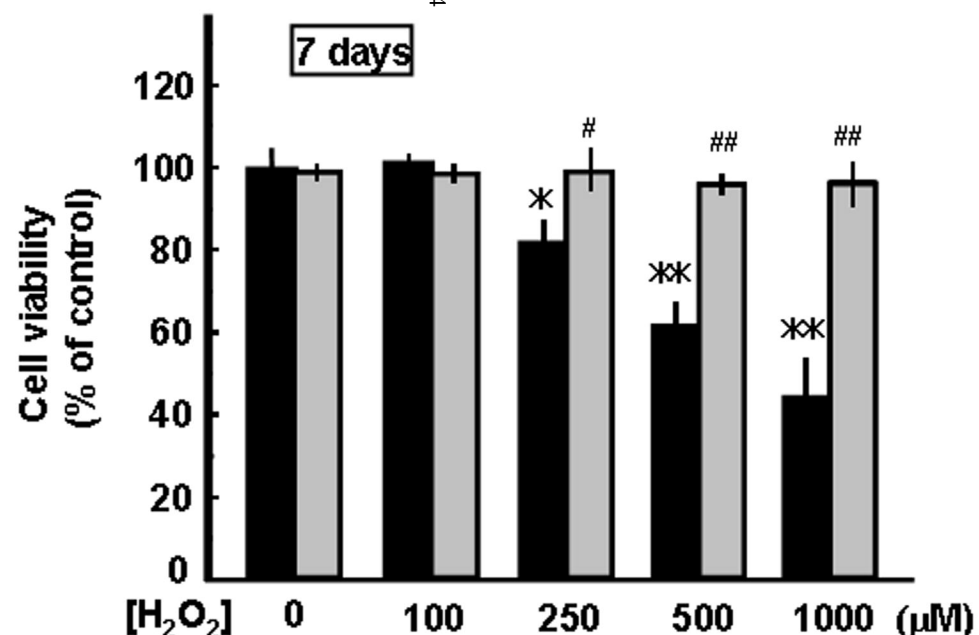
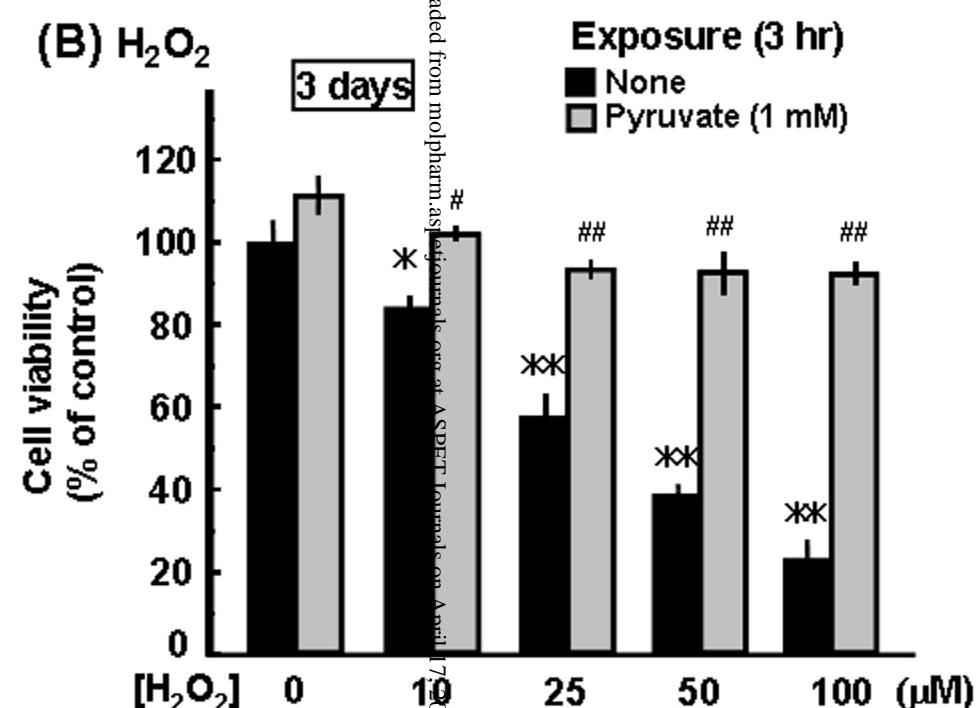
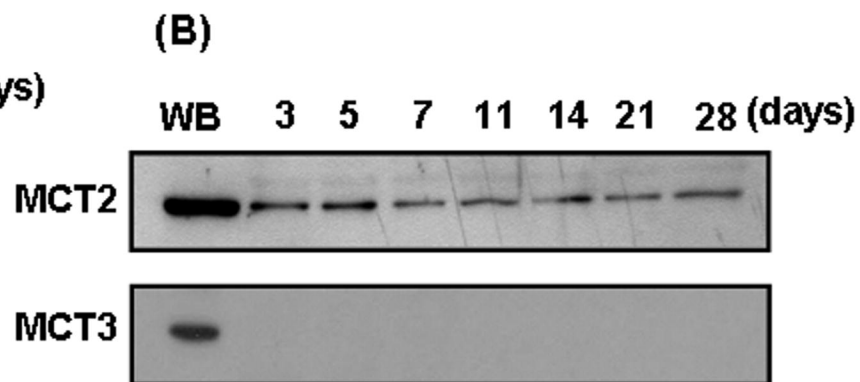
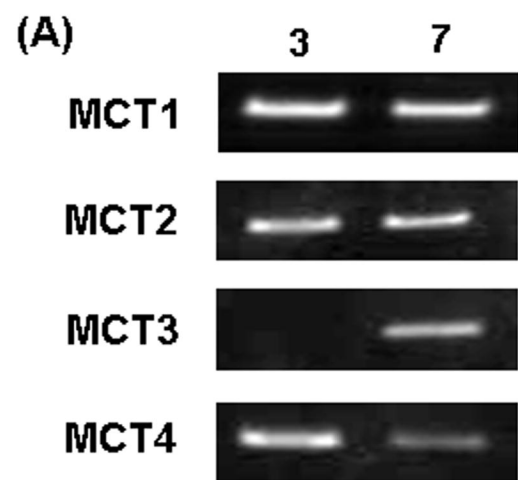
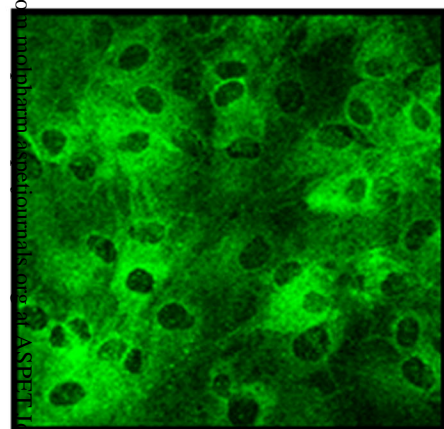
Fig. 1**(A) Menadione****(B) H₂O₂**

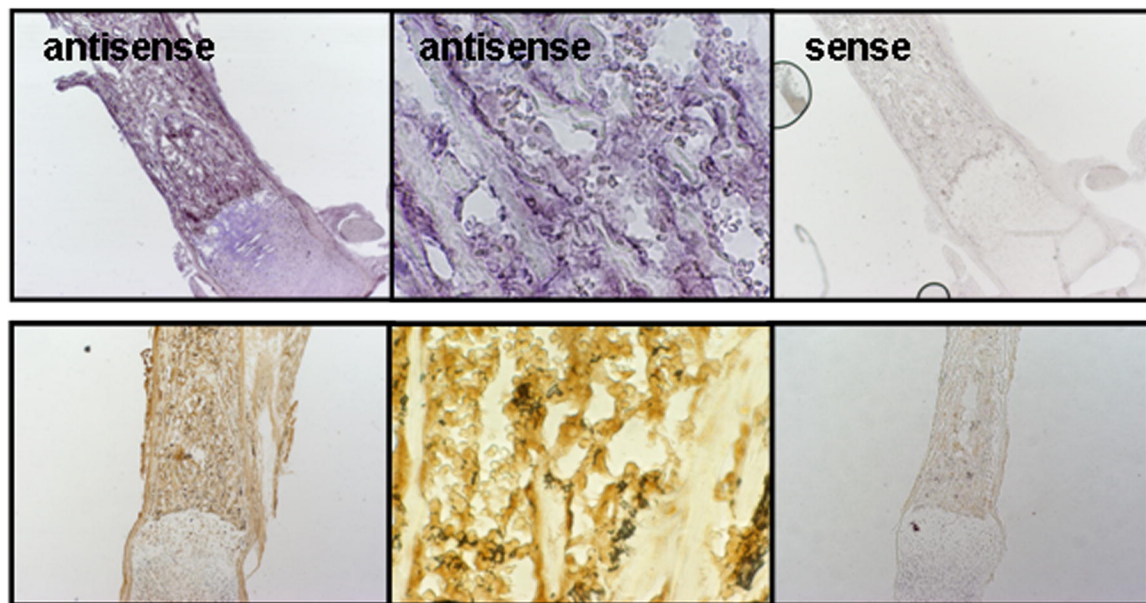
Fig. 2



(C) MCT2

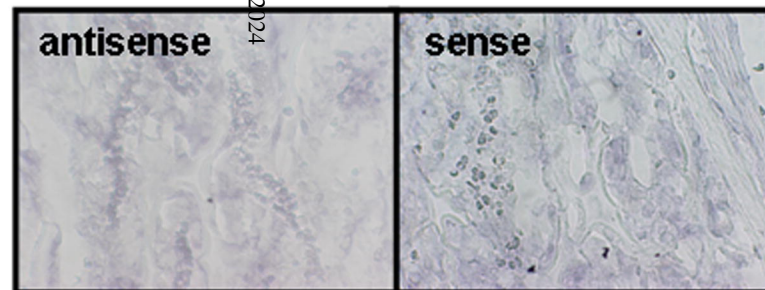


(D) MCT2



(E)

MCT1



MCT3

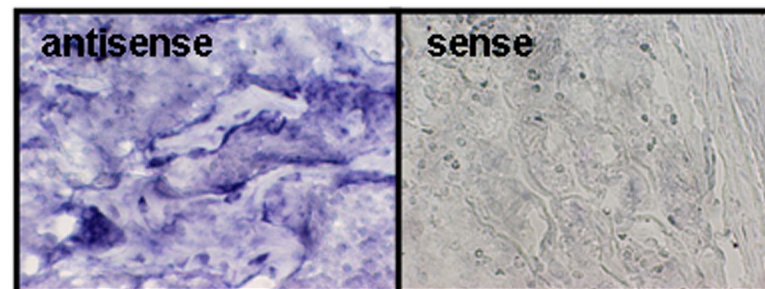


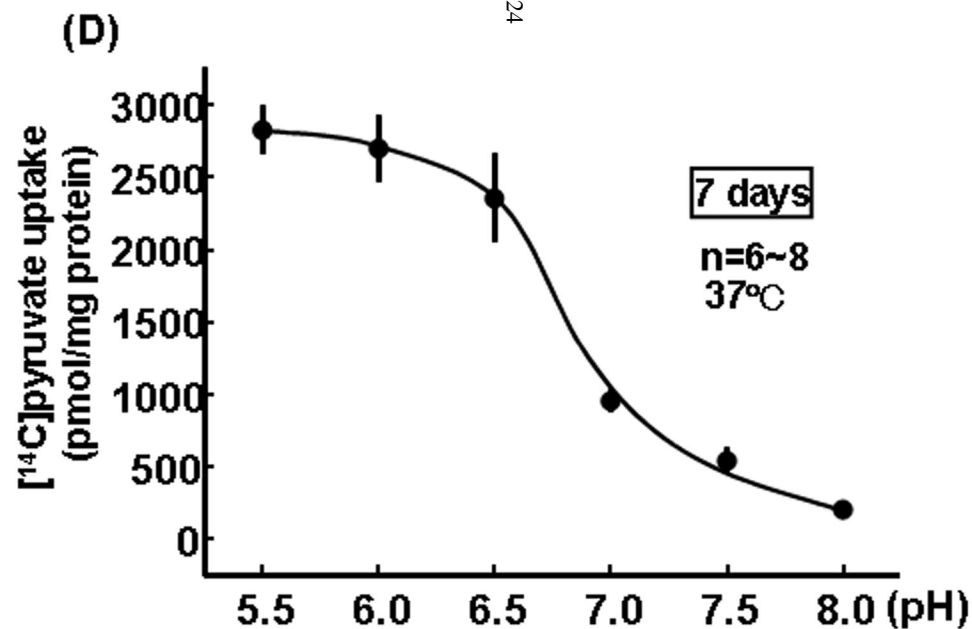
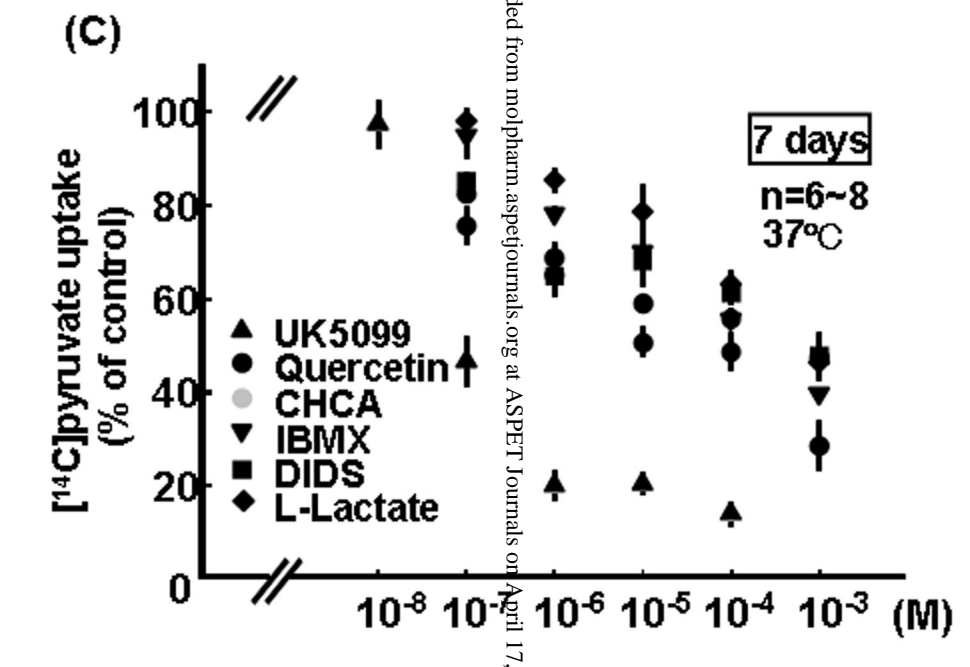
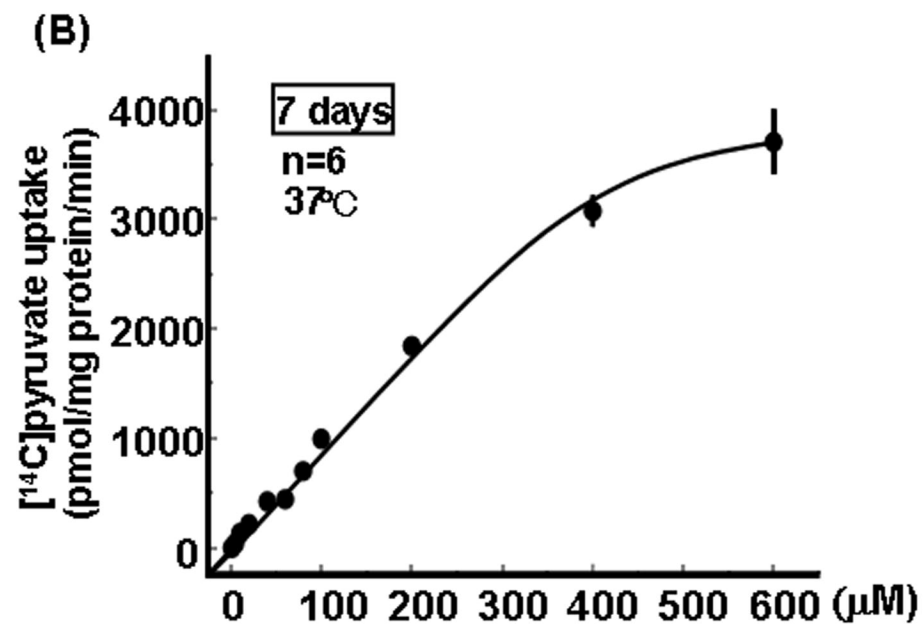
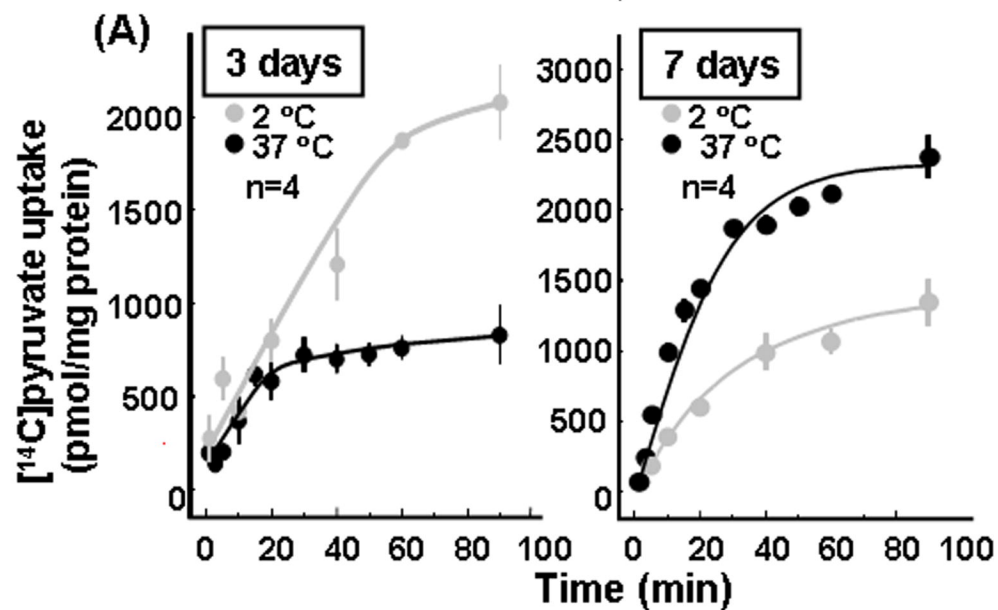
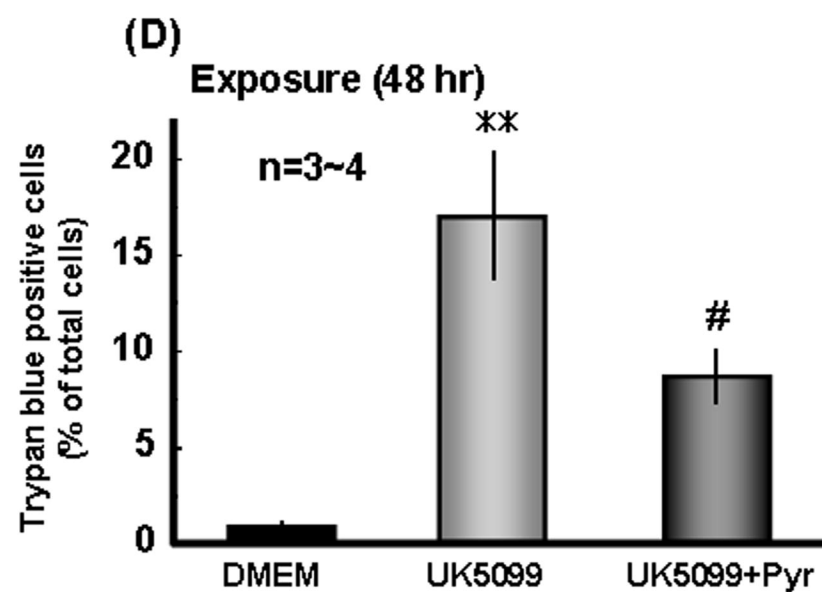
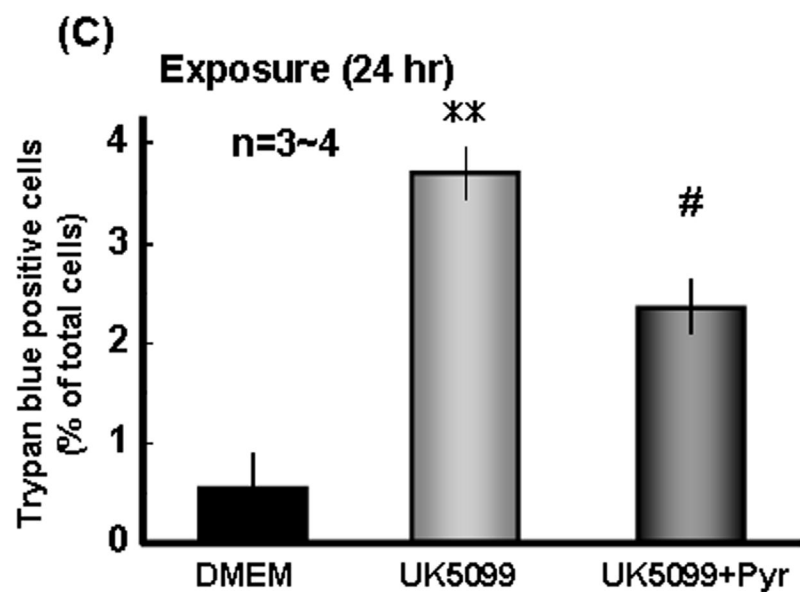
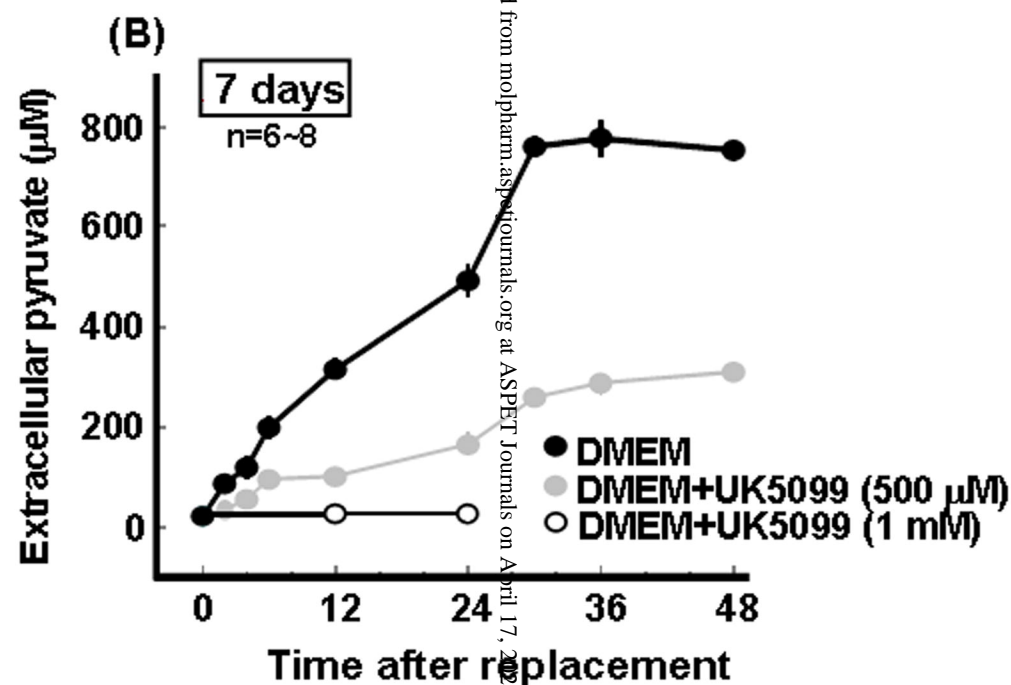
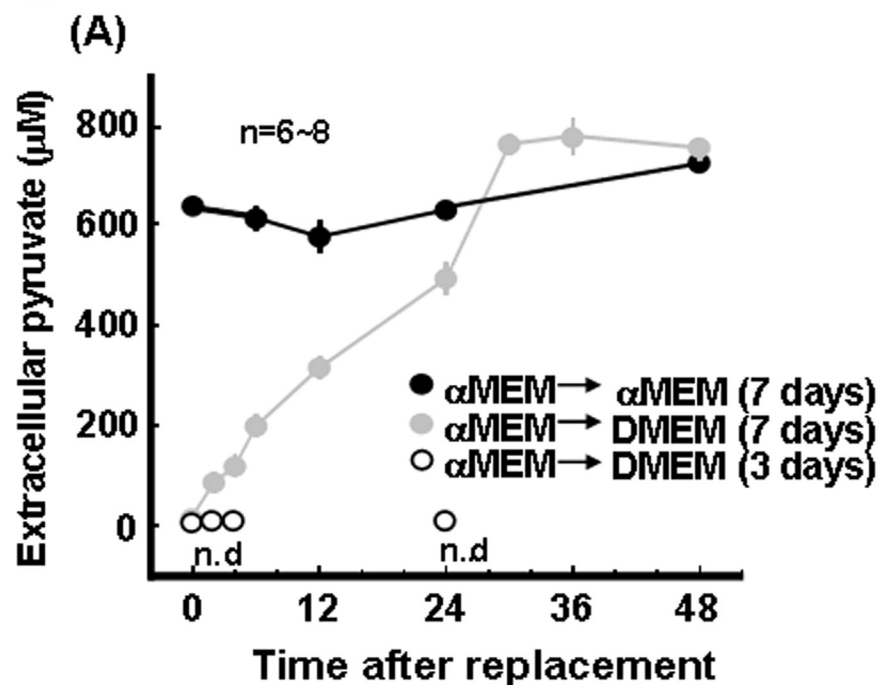
Fig. 3

Fig. 4

Downloaded from molpharm.aspenjournals.org at ASPET Journals on April 17, 2014

Fig. 5

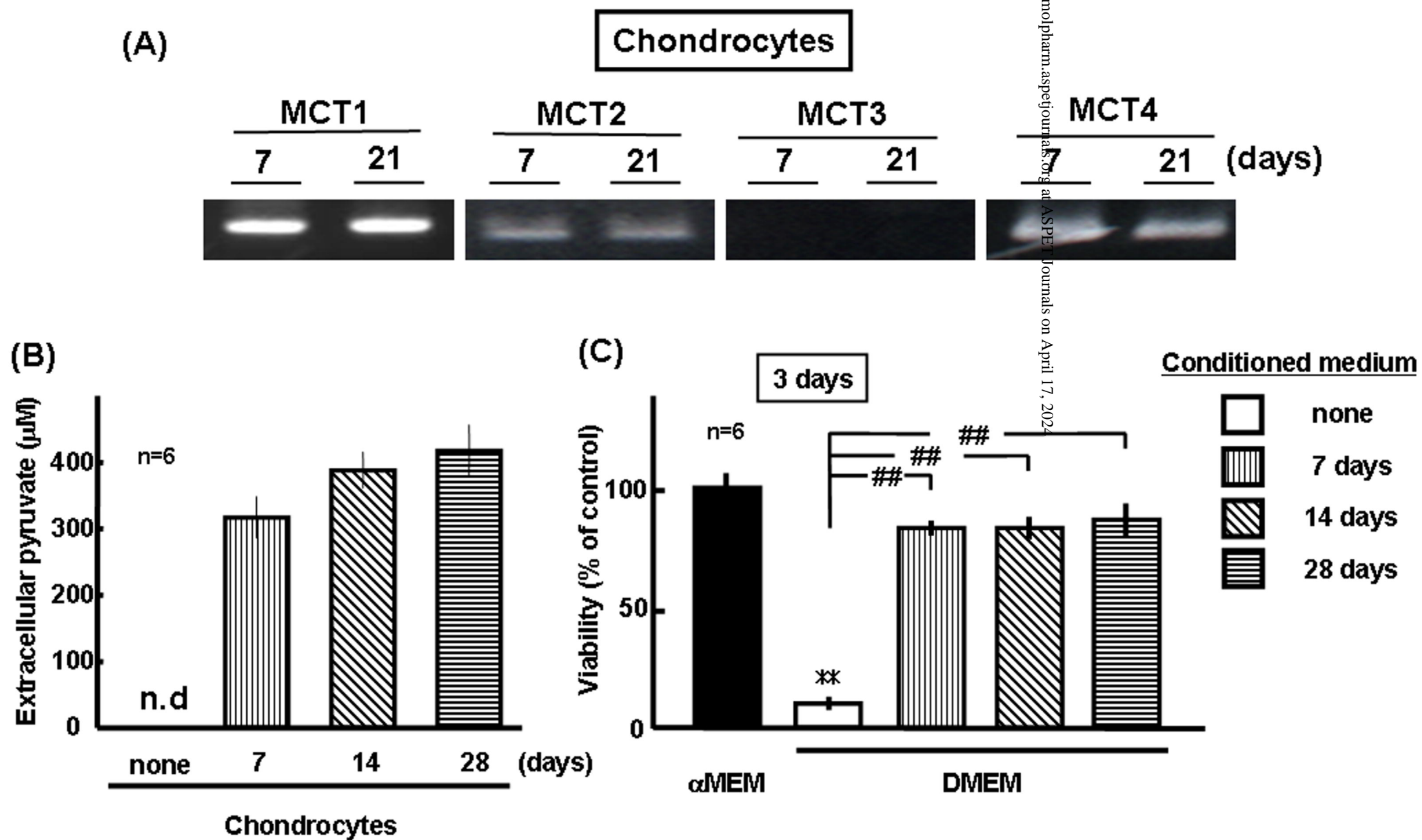


Fig. 6

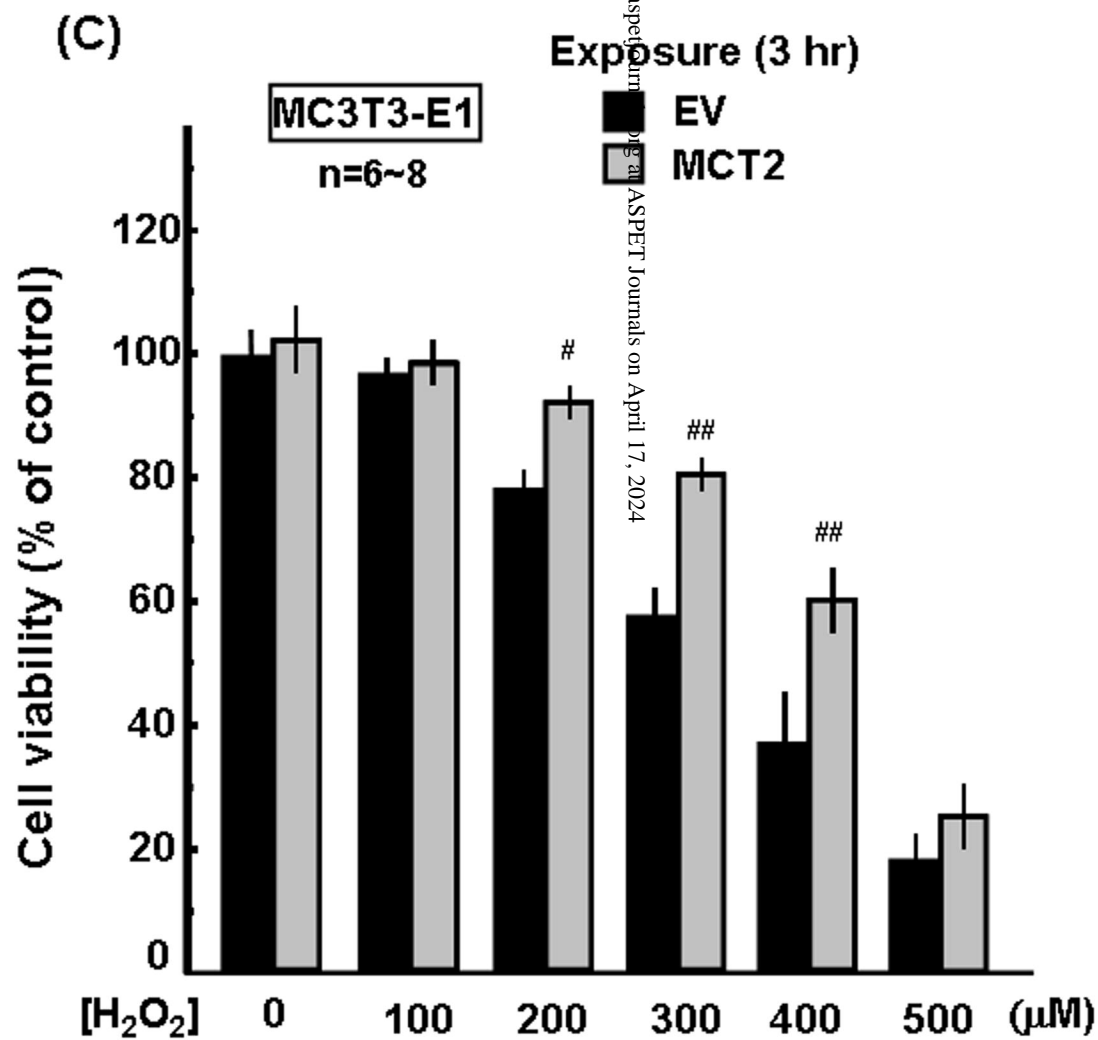
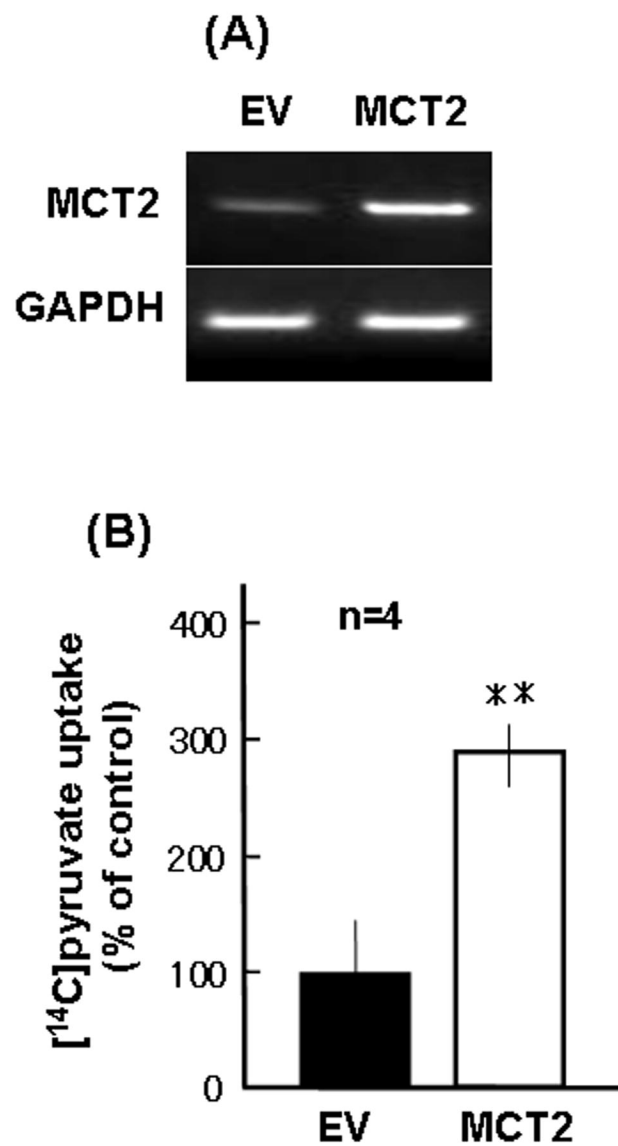
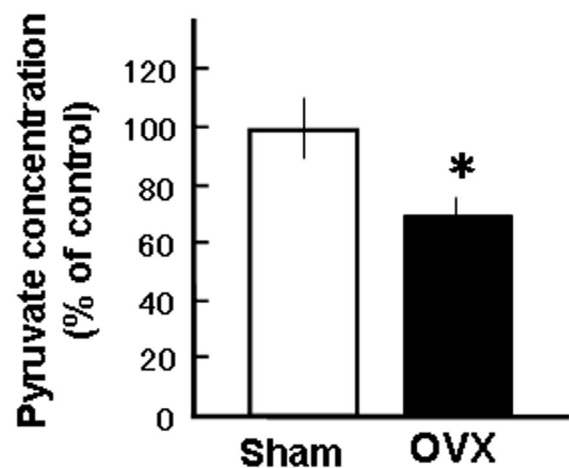
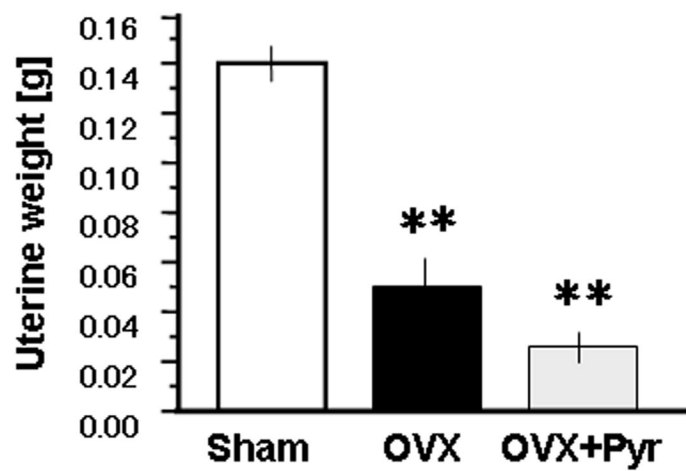


Fig. 7

(A)



(B)



(C)

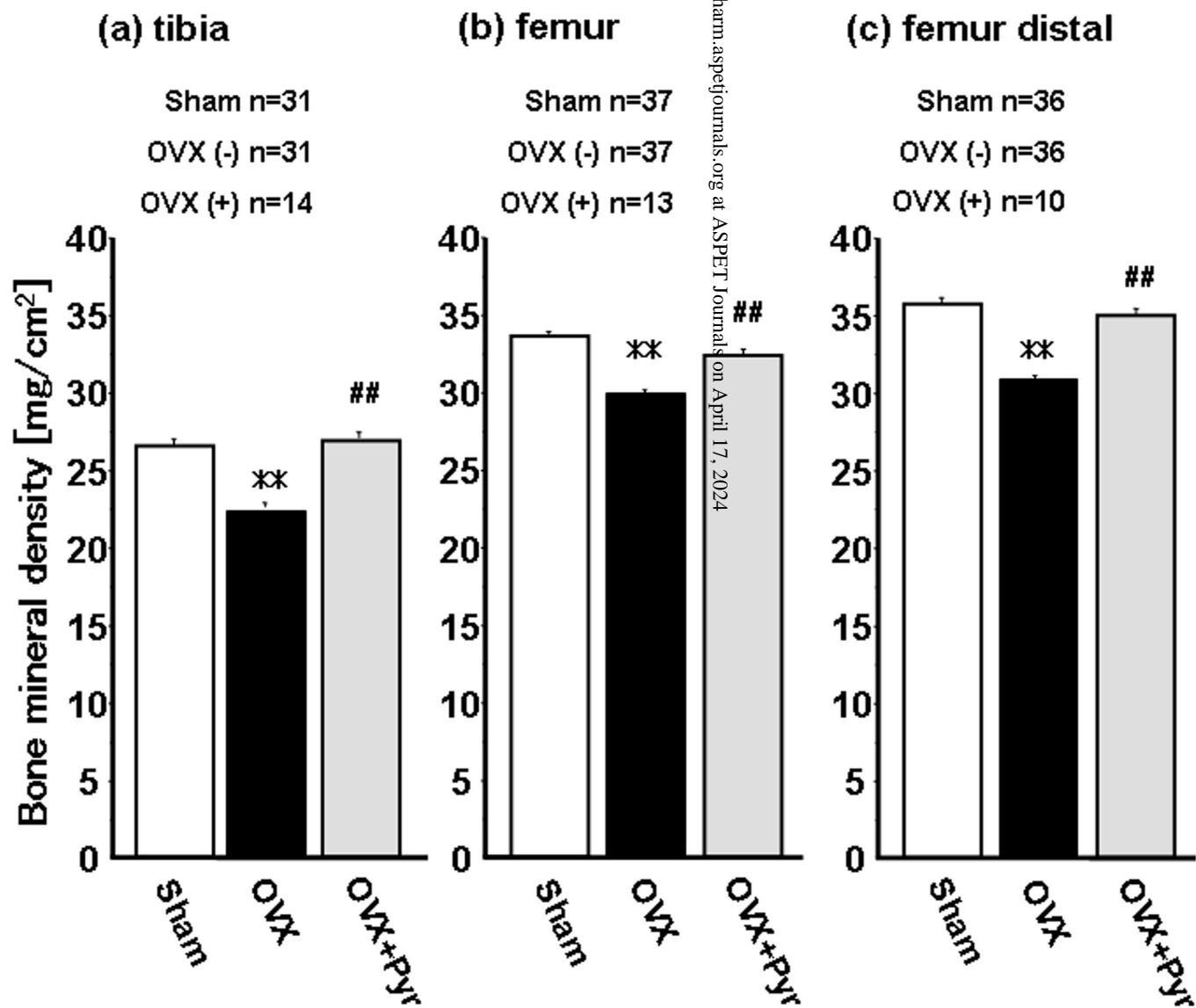
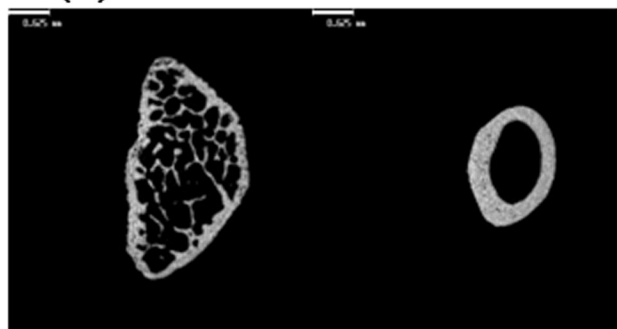


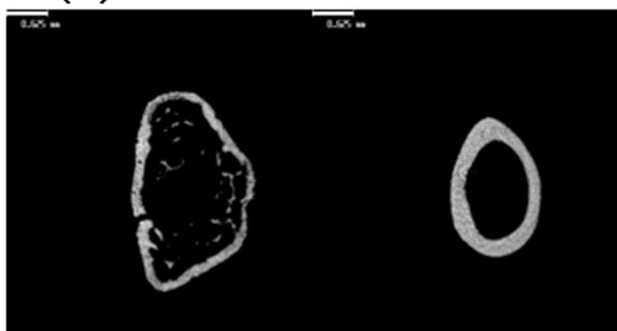
Fig. 8

(A)

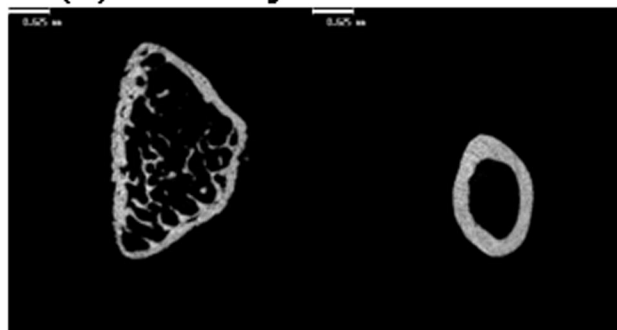
(a) Sham



(b) OVX

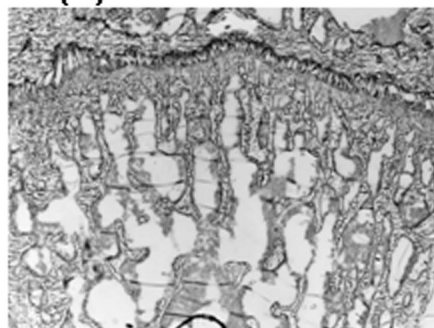


(c) OVX+Pyr

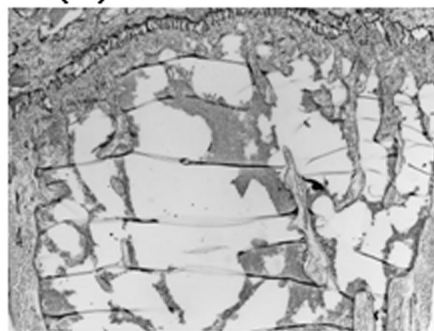


(B)

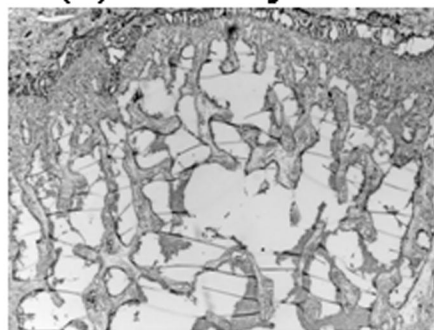
(a) Sham



(b) OVX



(c) OVX+Pyr



(C)

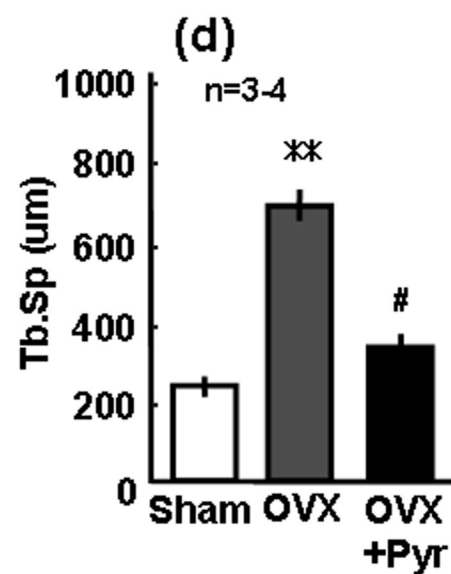
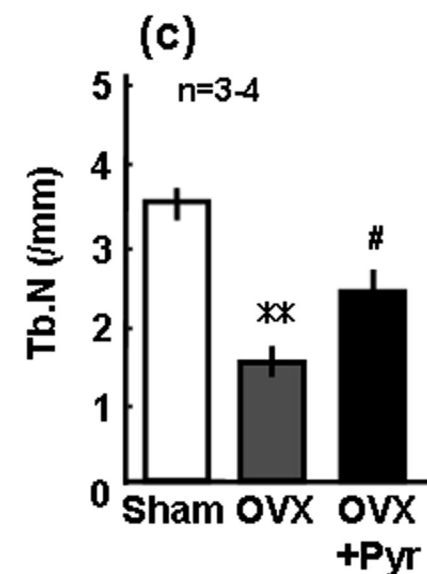
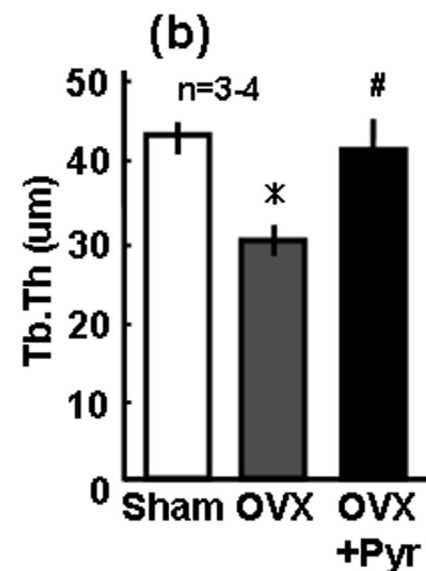
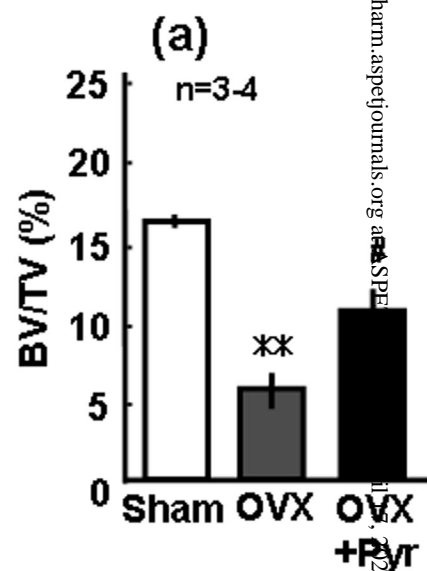


Fig. 9

Schematic model

